



Deposited via The University of Sheffield.

White Rose Research Online URL for this paper:

<https://eprints.whiterose.ac.uk/id/eprint/144265/>

Version: Accepted Version

---

**Proceedings Paper:**

Falconer, S.E., Taylor, Z.A. and Tomlinson, R.A. (2019) Developing a soft tissue surrogate for use in photoelastic testing. In: Vergani, L. and Guagliano, M., (eds.) *Materials Today: Proceedings*. 1st International Conference on Materials, Mimicking, Manufacturing from and for Bio Application, 27-29 Jun 2018, Milan, Italy. Elsevier, pp. 537-544. ISSN: 2214-7853. EISSN: 2214-7853.

<https://doi.org/10.1016/j.matpr.2018.12.005>

---

Article available under the terms of the CC-BY-NC-ND licence  
(<https://creativecommons.org/licenses/by-nc-nd/4.0/>).

**Reuse**

This article is distributed under the terms of the Creative Commons Attribution-NonCommercial-NoDerivs (CC BY-NC-ND) licence. This licence only allows you to download this work and share it with others as long as you credit the authors, but you can't change the article in any way or use it commercially. More information and the full terms of the licence here: <https://creativecommons.org/licenses/>

**Takedown**

If you consider content in White Rose Research Online to be in breach of UK law, please notify us by emailing [eprints@whiterose.ac.uk](mailto:eprints@whiterose.ac.uk) including the URL of the record and the reason for the withdrawal request.

# **DEVELOPING A SOFT TISSUE SURROGATE FOR USE IN PHOTOELASTIC TESTING**

S. E. Falconer, Dr Z. A. Taylor, Dr R. A. Tomlinson

*The University of Sheffield, Western Bank, Sheffield, S10 2TN, United Kingdom*

## **ABSTRACT**

An improved skin tissue substitute for use in photoelastic testing is required to enable investigation of the mechanics of needle insertion into soft tissue. Current tissue substitutes are mainly used in large scale testing and can neglect the small scale mechanical properties of soft tissue. A series of experiments on konjac glucomannan are performed to characterise its mechanical properties, and the results are compared to published results from similar experiments on skin tissue. The optical properties of the gel, such as its strain optic coefficient, are also assessed using a grey field polariscope (GFP2500).

A concentration of 1.5% konjac to water produced a viscoelastic gel whose mechanical response closely matches published data for skin. A strain optic coefficient was recorded and found ideal for the planned testing with a GFP2500. Overall konjac glucomannan was found to be a potential soft tissue surrogate for use in small scale photoelastic testing.

# 1 INTRODUCTION

Investigating the interaction between needles and tissues has been the topic of many researchers in recent years [1]. Many materials have been developed to replicate the properties of tissue, such as ballistic gel and silicone. These are commonly used for large scale testing and therefore can neglect the small scale properties of tissue [2], such as its resistance to crack growth and viscoelastic nature, which greatly affect a needle's trajectory. Consequently existing research has mainly composed of comparative analysis, due to the complexity of simulating human skin tissue [3].

## 1.1 Material Requirements

A skin tissue surrogate must reflect the mechanical properties of human skin tissue, such as its viscoelastic nature and approximate elastic modulus. A sample range of 0.0045 MPa – 0.85 MPa was found for average elastic modulus *in vivo* [4-11]. This is a large range so the average maximum and minimum values for elastic modulus were calculated in order to create a confined range which would better reflect the average properties; 0.10 – 0.27 MPa. Consequently, the elastic modulus for the surrogate tissue should fall within this range. As photoelasticity will be used to analyse the effects of needle insertion, the material must also be transparent and exhibit temporary birefringence.

In their research on needle interaction Okamura *et al.* [12] [13] used experiments to identify theoretical models of force involving material stiffness, friction, and cutting. Their study indicates that the total force acting on the needle can be divided into three components: cutting force, stiffness force, and friction.

$$F_{needle}(x) = F_{cutting}(x) + F_{stiffness}(x) + F_{friction}(x), \quad (1)$$

where  $F_{cutting}$  is the force required to continue tissue fracture,  $F_{stiffness}$  is the resultant force from tissue deformation, and  $F_{friction}$  exists between the needle and tissue due to the tissue's clamping effect. When skin is punctured with a needle the surrounding tissue doesn't tear; the material clings to the needle which produces the aforementioned friction force.

A recent report described the difficulty in finding a suitable material that doesn't tear when punctured with a needle [3]. Figure 1 displays the differences between the tissue clinging and tissue tearing.

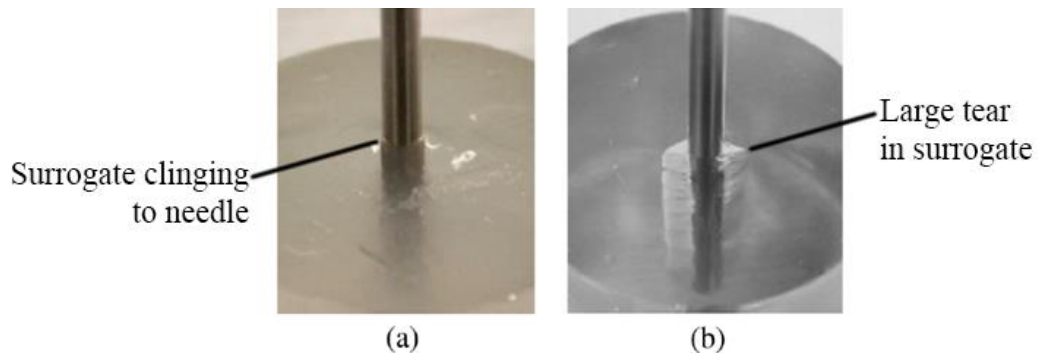


**Figure 1 (a) Gel that clings to punctured needle (b) Gel that exhibits tearing [3].**

It can be seen that when the tissue surrogate tears parts of the needle are not in contact with the material; the material is not clamping down on the needle like Okamura describes [14]. As a result of this the friction force experienced would be less than the friction caused from inserting the needle into real skin tissue. It is also assumed that the torn sections would constrain the movement of the needle to a specific plane. This may result in a different extent of deflection than the needle would experience when travelling through human skin tissue.

## **1.2 Photoelasticity**

Photoelasticity relies on the phenomenon of temporary birefringence, wherein polarised light enters a loaded material and splits along the two different indices of refraction in perpendicular directions. The two light waves travel at vectors parallel to the principal stresses, and at speeds proportional to the principal strains. Since the light travels at different speeds the two beams will exit the material at different times. One beam is essentially travelling behind the other; this results in a phase difference or retardation between the beams. If the light passes through a second polariser, this retardation can be observed in the form of interference or fringe patterns. The fringe patterns can be used to calculate the magnitude and orientation of the principal stresses. As soon as the material is unloaded, its birefringence will cease, and no fringe patterns will be observed.

Photoelasticity is usually described as a stress analysis technique, but for the purpose of this investigation the optical properties will be characterized through strain. Viscoelastic materials exhibit “stress relaxation”, in which stress decreases over time when the material is subject to a constant strain. During the following experiments the gels are held in rigid grips and any strain is recorded within known boundaries. Therefore it is more meaningful and accurate to express the optical characteristics through the strain optic law:

$$(\varepsilon_1 - \varepsilon_2) = \frac{Nf_\varepsilon}{t}, \quad (2)$$

where  $\varepsilon_1$  and  $\varepsilon_2$  represent the principal strains,  $N$  is the fringe order,  $f_\varepsilon$  is the strain optic coefficient in terms of strain, and  $t$  the thickness.

Since the developed material is viscoelastic the experimental techniques used must ensure that stress relaxation does not occur in the time taken to record data, as it could cause anomalous results. The collection of the resultant retardation is usually discontinuous process as the capture of full-field data requires the output polariser to be rotated, and the experiment in turn to be paused to capture data. At least four different orientations are required to gather a full field retardation map [15]. This rotation is undesirable as the time it takes to rotate the optical elements would allow for stress relaxation.

In order to avoid this issue a GFP2500 poleidoscope, developed by Stress Photonics Inc., will be used. This apparatus has the same optical elements as a normal polariscope setup but within the system it has an array of lenses which split the light beam four ways [15]. The four beams travel through the four required output polarizer orientations and therefore capture the full field data in a single image.

The work described in this paper involves three aspects: developing a surrogate which reflects the complex mechanical properties of skin tissue, developing test methods to characterise the mechanical properties, and characterizing the optical properties of the material.

## **2 MATERIAL DEVELOPMENT**

Konjac glucomannan is an amorphous polymer. It's derived from plants and used as a food thickening agent to make transparent jellies. A recent report showed that when a needle punctures konjac gel it produces a different puncture crack than conventional gels [3]; it does not tear and resists crack formation. The following section describes the development of konjac jelly as a suitable skin tissue surrogate. The results from the tensile tests were compared to ballistic gelatin, a gel that is commonly used as a tissue surrogate.

### **2.1 Material preparation**

The following work used a preparation of 1.5% konjac gel to water weight. The preparation of konjac jelly is as follows:

- The water and gel powder were measured on a digital scale and mixed together until homogenised in a gastronorm; a large rectangular container used in a bain-marie.
- The mixture was covered and left for a twenty-four hour period to allow for the gel powder to absorb the water.
- The gastronorms were placed in a wet-heat bain-marie and the temperature was set at 70°C.
- The gel was left to heat for one hour, and part way through it was shaken to promote even heat distribution.
- The gel was then carefully decanted into moulds and left to cool at room temperature for 24 hours.
- The solidified gel was removed from the moulds and placed in a refrigerator at  $4\pm 1^\circ\text{C}$  to set.
- After setting overnight, the gel was ready to test. It was kept refrigerated until required for testing. It can be stored up to three days, after which it begins to decompose. To promote consistency all the tests were carried out after 24 hours of setting time.

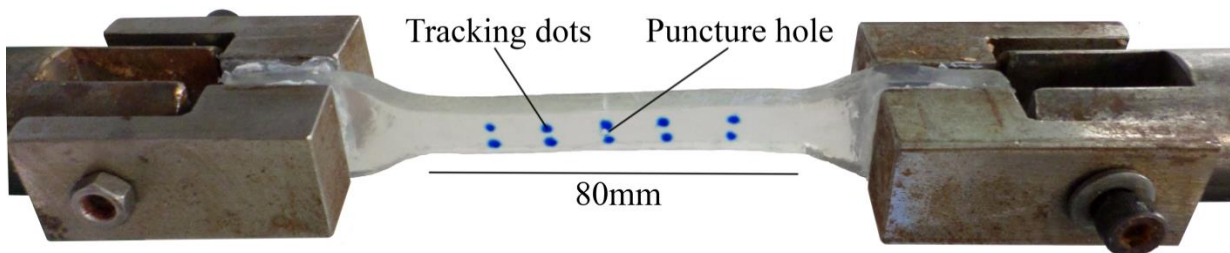
The preparation for the ballistic gelatin samples followed the same steps except it was heated at 50°C.

### 3 MECHANICAL CHARACTERIZATION

Tensile tests were performed to assess the gels resistance to tearing and elastic modulus in tension. Compression tests were also performed to assess the gels viscoelasticity and elastic modulus in compression.

#### 3.1 Tensile Tests

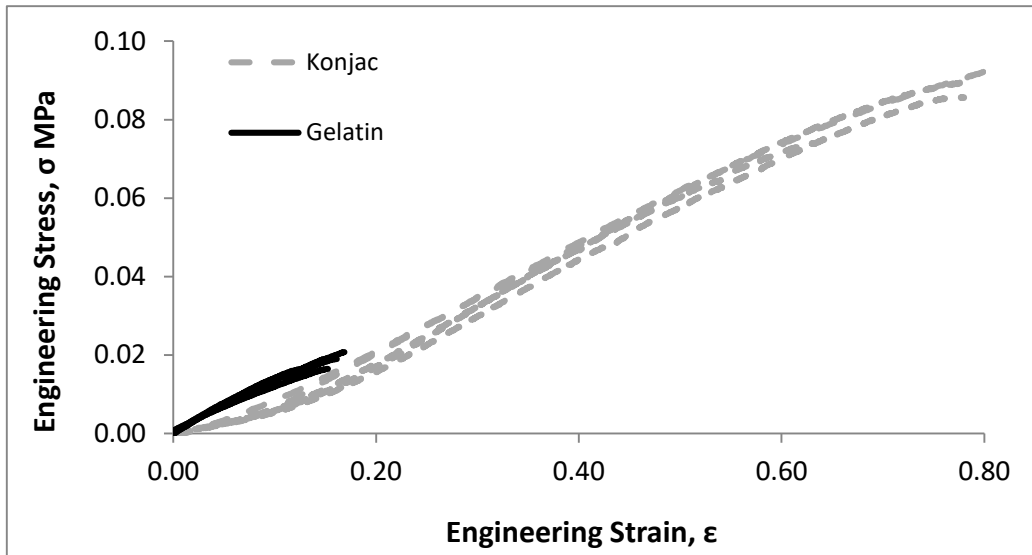
The molten gel was poured into moulds which match the sample shape for the standard ASTM D-412-F, which is a test standard for rubber and elastomers. The standard was adapted to include a needle puncture hole in the middle of the specimen, which made it possible to monitor the crack propagation from a needle insertion. As can be seen in Figure 2, the samples were glued to specially designed grips following work by Miller et al. [16]. This was to avoid gripping the samples through pressure and damaging the fragile material.



**Figure 2 Sample glued between grips with visible needle puncture and tracking dots**

Uniaxial tension tests were performed at an ambient temperature of  $24\pm 1^\circ\text{C}$ . The samples were refrigerated at  $4\pm 1^\circ\text{C}$  until they were required for testing. Once removed, they were quickly loaded into the grips and testing began to prevent heat absorption. The samples had a uniform cross section of  $8\times 6\text{mm}$  along its gauge length. Tests were performed with a constant loading speed of  $20\text{ mm/min}$ , and the corresponding retardation was captured using a GFP2500 poleidoscope.

As can be seen in Figure 2, the samples had opaque ink dots drawn on prior to testing. These dots were placed in a uniform orthogonal pattern with spacing of  $3\text{mm}$  and  $10\text{mm}$  in width and length directions, respectively. The gradual change in spacing between the dots allowed for estimation of the principal strain development. The test was filmed and the estimation was performed using the recordings. These data were used later in the optical analysis to calculate the strain optic coefficient of the material.



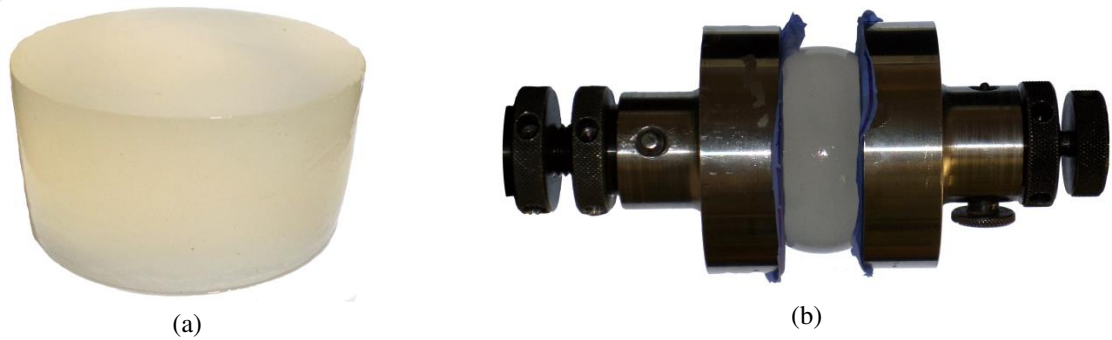
**Figure 3 Stress strain graph comparing the response from konjac gel (grey dotted line) and ballistic gelatine (black solid line)**

Figure 3 shows the developing stress strain curves for konjac and ballistic gelatin; four of each gel type were tested and displayed. The effect of the resistance to crack growth (or tearing) is reflected in this curve by the differences in fracture location. The area under the curve represents the toughness of the two materials; it is clear that konjac jelly is the tougher of the two materials and hence has a greater resistance to crack growth.

The elastic modulus for the konjac jelly was calculated using the gradient of the curve in the linear section between 0.2 and 0.5 strain. This does ignore the small non-linear section but this research is interested in the crack development where a large strain is required for a crack to form. The elastic modulus for konjac jelly of 1.5% powder to weight was found to be  $E = 0.113 \pm 0.004$  MPa.

### **3.2 Compression tests**

Compression tests were also conducted to assess the material's elastic modulus in compression and viscoelastic response. Moulds were used to create cylindrical specimens of 50mm diameter and 20mm height.



**Figure 4 (a) Image of compression sample (b) Image of sample between compression grips at 0.25 strain – Image rotated 90°**

The samples were glued to the grips for testing in order to prevent them from slipping. It is evident from Figure 4 (b) that barrelling does occur; at a strain of 0.25 the maximum diameter has increased by 5mm. While this is a significant increase and will affect the recorded properties of the material, the in vivo experiments used to characterise skin tissue also overlooked the effects of barrelling. In order to produce a relevant material comparison between the konjac gel and skin tissue it is logical to ignore the effects of barrelling for now.

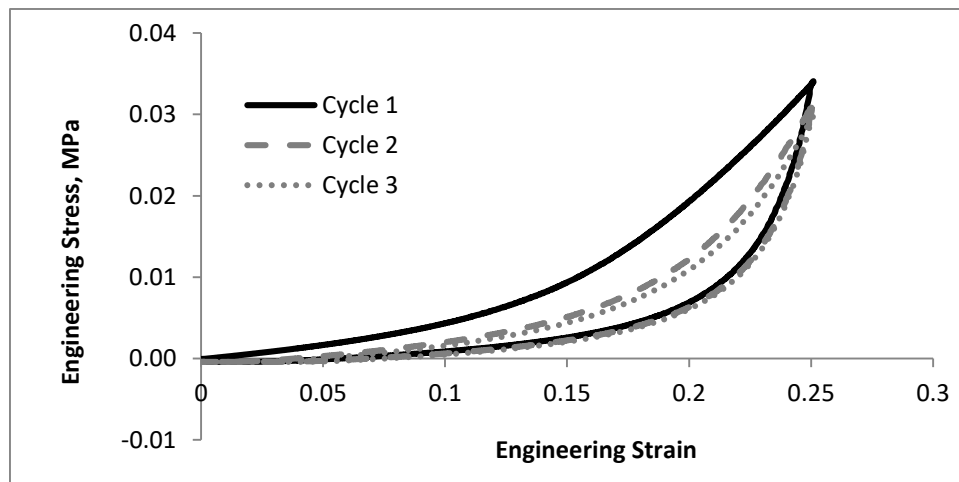


**Figure 5 Cyclic compression response of konjac jelly**

Figure 5 shows the response of the material under 20 mm/minute cyclic compression for three cycles up to a strain of 0.25. It can be seen that the material undergoes a preconditioning phase during the first cycle, and subsequent cycles adhere to a tighter sequence. A similar behaviour has been observed in porcine skin in a study by Remache et al [17].

Since the purpose of this surrogate material is for needle insertion investigation, the mechanical properties of the gel will be estimated using the initial cycle. This is because it is highly unlikely the area of needle insertion on a patient will be preconditioned prior to a puncture, so using the material when it is also unconditioned is more meaningful.

Once more, the elastic modulus for the konjac jelly was calculated using the slope of the curve in the linear section between 0.2 and 0.25 strain. Similar to the tensile tests the elastic modulus was calculated in this section because this research is interested in the crack development where a large strain is required for a crack to form. The elastic modulus for konjac jelly of 1.5% powder to weight was found to be  $E = 0.264 \pm 0.018$  MPa.

#### 4 OPTICAL CHARACTERISATION

Photoelastic testing with this material requires the determination of a strain optic coefficient. Uniaxial tension tests were performed in the same way as described earlier. Tests were performed with a constant loading rate of 20mm/min, and results were recorded using a GFP2500 which allowed for instantaneous capture of the full field retardation map.

Samples were elongated by a total length of 20mm and images were processed at 5mm intervals. Using the Stress Photonics software [18] the retardation was recorded for each of these extension lengths. The progression of the retardation is shown in Figure 6.

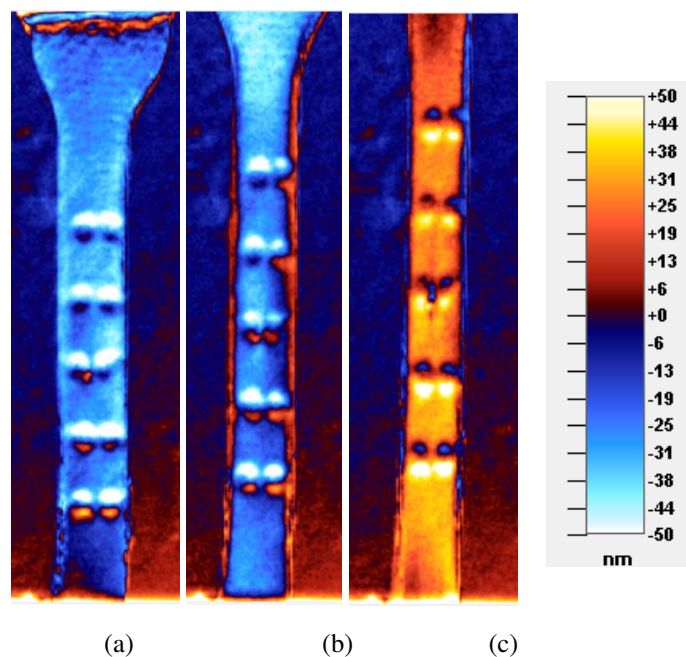


Figure 6 Processed results showing the development of the retardation during extension; a) 0mm, b) 10mm, c) 20mm extension

Conventionally fringe order is used to calculate strain optic coefficient, yet in the following calculation the retardation in the mid-section was used. This is because the Stress Photonics software returns fringe orders in increments of 0.25, and in this case the maximum fringe order was 0.75. This incremental increase prevented a precise calculation of strain optic coefficient so retardation was used instead.

$$N = \frac{\delta}{2\pi} \quad (3)$$

The above equation describes the relationship between fringe order,  $N$ , and retardation,  $\delta$ . Combining equations (2 and (3 returns a calculation for strain optic coefficient in terms of retardation.

$$f_{\varepsilon} = \frac{(\varepsilon_1 - \varepsilon_2)2\pi t}{\delta} \quad (4)$$

The local longitudinal and lateral strain were also captured and calculated for each of the intervals by measuring the change in distance of the opaque ink dots during extension. Assuming the y-axis is coincident with the loading of the tensile specimens, these data were used in equation (4 to calculate the strain optic coefficient of the material:  $f_{\varepsilon} = 0.56 \pm 0.07$  mm/fr.

## 5 DISCUSSION

In order to be an effective skin tissue surrogate for use in assessing needle deflection through soft tissue three main requirements needed to be met:

**Stiffness:** Previously, a sample range of 0.10 MPa – 0.27 MPa was established for *in vivo* elastic modulus of skin [4-11]. Tensile and compression tests were used to estimate the elastic modulus of konjac jelly of 1.5% powder to water weight. The results varied greatly for each type of experiment; tensile tests returned an elastic modulus of  $0.113 \pm 0.004$  MPa. and the compression experiments resulted in a higher value of  $0.264 \pm 0.018$  MPa. These values lie on either end of the established range for skin.

Skin tissue tested *in vivo* also exhibited a significant difference for elastic modulus between compressive and tension experiments. Tension experiments by Paillet-Mattei et al. indicated an elastic modulus range of 0.0045 - 0.0080 MPa [9]. These results vary significantly compared to the compressive response of skin tissue through indentation testing by Khatyr et al. who indicated an elastic modulus range of 0.13 - 0.66 MPa [7], while Jachowicz et al. reported a range of 0.007 – 0.033 MPa [8].

It is theorised that the difference in recorded mechanical properties for tension and compression could be a result of the fibrous nature of skin tissue. The collagen fibers may behave differently when subjected to tensile and compressive loads. No matter the causes for this observed diverse response, it is ideal that the developed gel also exhibits a similar response so future mechanical testing will be more meaningful.

**Tear Resistance:** The importance of a material which does not tear was discussed within this paper, as it changes the force profile and potentially alters the needle trajectory. Previous work at the University of Sheffield showed that when a needle punctures konjac gel it produces a different puncture crack than conventional gels [3], namely ballistic gelatin. This was investigated further here by assessing the toughness of the gels using tensile testing with an initial puncture hole to assess the crack propagation. It was found that konjac jelly exhibited a significantly higher toughness than conventional gels and thus its resistance to crack growth better emulates that of skin tissue.

**Optical Properties:** The optical properties of the konjac jelly are also ideal: it is possible to manufacture an optically clear jelly which also exhibits temporary birefringence; thus, it is suitable for use in photoelastic testing. A strain optic coefficient of  $f_{\epsilon} = 0.56 \pm 0.07$  mm/fr was calculated using the strain optic law and utilising a combination of digital image correlation and photoelastic analysis.

With comparison to strain optic coefficients in literature it is found that strain optic coefficient decreases with increasing stiffness [19]. This calculated value fits into this trend with a reasonably high strain optic coefficient and low stiffness. This strain optic coefficient will produce low fringe orders, yet the GFP2500 works best with a fringe order between 0 and 2.5, so this value is beneficial for the planned analysis techniques.

## 6 CONCLUSION

Experimental research was presented on the viability of using konjac jelly as a skin tissue surrogate for use in needle insertion investigation. Experiments aimed at characterising the mechanical properties of the gel were described, and comparisons drawn to the published mechanical properties of human skin tissue *in vivo*. A concentration of 1.5% konjac to water produced a viscoelastic gel whose mechanical response closely matches published data for skin. Cyclic testing was also presented which showed how the gel exhibited a preconditioning phase, a phenomenon which has also been recorded in porcine skin tissue. It was found that the gel behaved differently under compressive and tensile testing, a behaviour that has also been observed in skin tissue.

Optical properties of the gel were also recorded to assess its viability for use in photoelastic testing. The gel was translucent and colourless, and exhibited temporary birefringence. The strain optic coefficient of the gel will produce low fringe orders, but this is ideal for the planned experiments using a grey field polariscope which works best at fringe orders under 2.5.

Future research will use this material to assess the developing strain field surrounding different needle tips. The various needle deflections caused by varying the tip shape will also be recorded.

### **Acknowledgements**

This work was supported by an EPSRC DTP studentship.

## REFERENCES

- [1] D. J. van Gerwen, J. Dankelman, and J. J. van den Dobbelsteen, "Needle–tissue interaction forces – A survey of experimental data," *Mechanical Engineering and Physics*, vol. 34, pp. 665-680, 2012.
- [2] R. A. Mrozek, Y. R. Sliozberg, J. W. Andzelm, and J. L. Lenhart, "Polymer Gels for Defense Applications," 2014.
- [3] R. Tomlinson and Z. Taylor, "Photoelastic materials and methods for tissue biomechanics applications," *Optical Engineering*, vol. 54, no. 8, p. 081208, 2015.
- [4] R. Sanders, "Torsional Elasticity of Human Skin in vivo," *Pflugers Arch*, vol. 342, pp. 255-260, 1973.
- [5] P. G. Agache, C. Monneur, J. L. Leveque, and J. De Rigal, "Mechanical Properties and Youngs Modulus of Human Skin in Vivo," *Dermatological Research*, vol. 269, pp. 221-232, 1980.
- [6] S. Diridollou *et al.*, "An in vivo method for measuring the mechanical properties of the skin using ultrasound," *Ultrasound in Medicine and Biology*, vol. 24, no. 2, pp. 215-224, 1998.
- [7] F. Khatyr, C. Imberdis, P. Vescovo, D. Varchon, and J. M. Lagarde, "Model of the viscoelastic behaviour of skin in vivo and study of anisotropy," *Skin research and Technology*, vol. 10, pp. 96-103, 2004.
- [8] J. Jachowicz, R. McMullen, and D. Prettypaul, "Indentometric analysis of in vivo skin and comparison with artificial skin models," *Skin Research and Technology*, vol. 13, pp. 299-309, 2007.
- [9] C. Pailler-Mattei, S. Bec, and H. Zahouani, "In vivo measurements of the elastic mechanical properties of human skin by indentation tests," *Medical Engineering & Physics*, vol. 30, no. 5, pp. 599-606, 2008.
- [10] H. Zahouani, C. Pailler-Mattei, B. Sohm, R. Vargiolu, V. Cenizo, and R. Debret, "Characterization of the mechanical properties of a dermal equivalent compared with human skin in vivo by indentation and static friction tests.," *Skin Research and Technology*, vol. 15, pp. 68-76, 2009.
- [11] X. Liang and S. A. Boppart, "Biomechanical Properties of In Vivo Human Skin from Dynamic Optical Coherence Elastography," *Transactions on Biomedical Engineering*, vol. 57, no. 4, pp. 953-959, 2010.
- [12] A. M. Okamura, C. Simone, and M. D. O'Leary, "Force Modeling for Needle Insertion Into Soft Tissue," *Transactions on Biomedical Engineering*, vol. 51, pp. 1707 - 1716, 2004.
- [13] Z. Cheng, M. Chauhan, B. L. Davies, D. G. Caldwell, and L. S. Mattos, "Modelling needle forces during insertion into soft tissue," presented at the EMBC, 2015.
- [14] A. M. Okamura, C. Simone, and M. D. O'Leary, "Force Modeling for Needle Insertion Into Soft Tissue," *Transactions on Biomedical Engineering*, vol. 51, pp. 1707-1716, 2004.

- [15] J. Lesniak, S. J. Zhang, and E. A. Patterson, "Design and Evaluation of the Poleidoscope A Novel Digital Polariscopes," *Society for Experimental Mechanics*, vol. 44, no. 2, pp. 128-135, 2004.
- [16] K. Miller, "How to test very soft biological tissues in extension?," *Journal of Biomechanics*, vol. 34, pp. 651-657, 2001.
- [17] D. Remache, M. Caliez, M. Gratton, and S. Dos Santos, "The effects of cyclic tensile and stress-relaxation tests on porcine skin," *Mechanical Behaviour of Biomedical Materials*, vol. 77, pp. 242-249, 2018.
- [18] "Stress Photonics." (accessed February, 2018).
- [19] J. W. Dally and W. F. Riley, *Experimental Stress Analysis*, 4 ed. Knoxville: College House Enterprises, 2005.